

DeepDetect: Learning All-in-One Dense Keypoints

Shaharyar Ahmed Khan Tareen
University of Houston
 Houston, TX, USA
 stareen@cougarnet.uh.edu

Filza Khan Tareen
National University of Sciences and Technology
 Islamabad, Pakistan
 ftareen.bse2021mcs@student.nust.edu.pk

Xiaojing Yuan
University of Houston
 Houston, TX, USA
 xyuan@uh.edu

Abstract—Keypoint detection is the foundation of many computer vision tasks, including image registration, structure-from-motion, 3D reconstruction, visual odometry, and SLAM. Traditional detectors (SIFT, ORB, BRISK, FAST, etc.) and learning-based methods (SuperPoint, R2D2, QuadNet, LIFT, etc.) have shown strong performance gains yet suffer from key limitations: sensitivity to photometric changes, low keypoint density and repeatability, limited adaptability to challenging scenes, and lack of semantic understanding, often failing to prioritize visually important regions. We present DeepDetect, an intelligent, all-in-one, dense detector that unifies the strengths of classical detectors using deep learning. Firstly, we create ground-truth masks by fusing outputs of 7 keypoint and 2 edge detectors, extracting diverse visual cues from corners and blobs to prominent edges and textures in the images. Afterwards, a lightweight and efficient model: “ESPNet”, is trained using fused masks as labels, enabling DeepDetect to focus semantically on images while producing highly dense keypoints, that are adaptable to diverse and visually degraded conditions. Evaluations on Oxford, HPatches, and Middlebury datasets demonstrate that DeepDetect surpasses other detectors achieving maximum values of 0.5143 (average keypoint density), 0.9582 (average repeatability), 338,118 (correct matches), and 842,045 (voxels in stereo 3D reconstruction).

Index Terms—keypoint detection, edge detection, image fusion, image matching, SIFT, ORB, deep learning, 3D reconstruction.

I. INTRODUCTION

Keypoint detection is the backbone of many computer vision applications including image matching, panorama stitching, object tracking, 3D reconstruction, visual odometry, and visual SLAM [1]. Keypoints (often referred to as features or feature points) are the distinctive points in an image that can also be identified to an extent under various transformations or degradations by the detectors. They are usually corners, blobs, ridges, and textured patterns that stand out from their surroundings [1]. Selection of keypoint detector is a critical decision in computer vision as it determines the stability, repeatability, map density, and overall performance of the downstream application [2]–[6]. A variety of detectors have been proposed over the years, ranging from traditional algorithms (SIFT, SURF, Harris Corner Detector, ORB, BRISK, and AGAST) to deep learning based approaches (SuperPoint, R2D2, D2-Net, Quad-Net, and LIFT). After keypoint detection, corresponding feature descriptors are computed by encoding the local pixel neighborhood around each keypoint into a distinctive vector

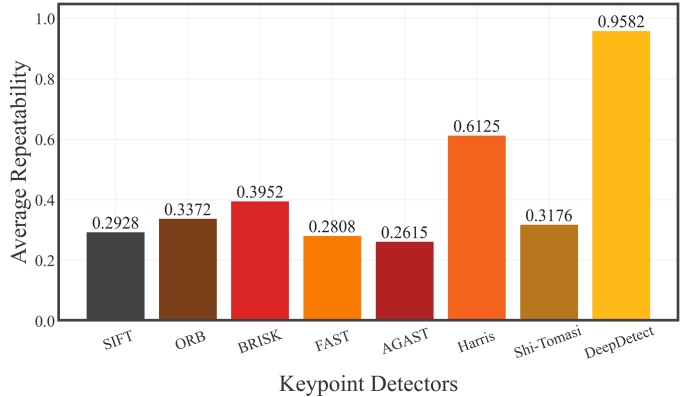


Fig. 1: Average repeatability of keypoint detectors on Oxford dataset [11].

that enhances stability across image variations [1]. A good descriptor is more distinctive and invariant to diverse image transformations or degradations [7]–[10].

After detection and description, “feature matching” is performed to match the descriptors and establish geometric relationships between the images [7]. NNDR is an effective matching strategy [12], that combines nearest neighbor search with a distance ratio test to reduce incorrect matches. The resulting matches are filtered by using model fitting algorithms: RANSAC [13], PROSAC [14], and MSAC to reject the outliers. Reliable image matching depends on the effectiveness of four stages: keypoint detection, keypoint description, feature (descriptor) matching, and outlier rejection [7], enabling robots or machines to accurately perceive, localize, and generate dense maps of their surroundings. Therefore, achieving high performance in the primary stage: **keypoint detection**, is crucial, as weaknesses at this stage propagate and lead to degradation in the performance of downstream tasks.

Classical detectors are invariant to different image transformations (scale, rotation, affine, blur) but sensitive to extreme variations (intense darkness, extreme photometric/geometric changes, severe smoke or fog) [8]. With standard settings, they detect sparse keypoints that inadequately cover texture-rich and low-contrast regions [8]. They also lack semantic understanding to prioritize important regions in the images.

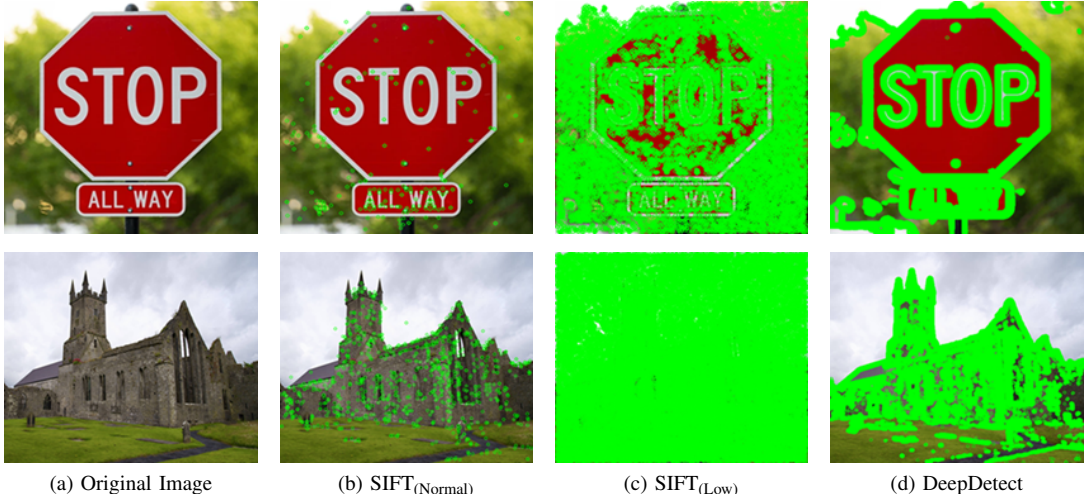


Fig. 2: Keypoint detection on two images using SIFT with normal (default) thresholds, SIFT with extremely low thresholds, and DeepDetect. Number of detected keypoints: Top Scene — 279, 23990, 46309 and Bottom Scene — 1009, 75465, 51115, respectively. SIFT with standard thresholds yields limited keypoints, whereas SIFT with extremely low thresholds produces high number of keypoints, detecting noisy features on semantically irrelevant regions. DeepDetect produces highly dense keypoints with substantially lower noise, well concentrated in semantically important regions of the images.

Learning-based detectors SuperPoint, R2D2, D2-Net, QuadNet, and LIFT) improve keypoint generalization and stability but their qualitative results show similar shortcomings [15]–[19]. They detect sparse keypoints and lack semantic awareness, potentially missing important regions in cluttered or low-visibility scenes [15]–[19]. This highlights the need for an intelligent and dense keypoint detector that is robust to complex image transformations and focuses on important regions.

Key Contributions: Our contributions are highlighted below:

- We present **DeepDetect**, an **intelligent, adaptable, all-in-one**, and **dense** keypoint detector that uses deep learning to learn the strengths of 7 strong keypoint detectors (SIFT, ORB, BRISK, FAST, AGAST, Harris Corner Detector, and Shi-Tomasi Corners) and 2 well-known edge detectors (Canny and Sobel). It provides highly dense and semantically meaningful keypoints, demonstrating robustness to poor visibility and brightness, low contrast, and complex scenes, without requiring manual tuning (as in classical detectors).
- We name this novel concept of **keypoint-edge fusion** as **DeepDetect**, that generates rich and diverse supervision masks, which later on serve as labels for training.
- We use a lightweight, efficient model: “ESPNet”, to ensure that DeepDetect has a small memory footprint: **1.82 MB** and **0.41 M parameters**, making it well-suited for deployment on edge devices such as mobile phones.
- We demonstrate that DeepDetect outperforms other detectors both qualitatively and quantitatively by significant margins. DeepDetect provides highest performance across three different datasets, with an average repeatability of **0.9582** (Oxford), average keypoint density of **0.5143** (Oxford), **338,118** number of correct matches (HPatches), and as high as **842,045** voxels in 3D re-

construction (Middlebury), outperforming the classical detectors even when extremely low thresholds are used.

- The code of DeepDetect is available at the following link: <https://github.com/saktx/DeepDetect>

II. RELATED WORK

Classical feature detectors have laid the foundation of modern computer vision. However, they rely on handcrafted criteria such as gradient magnitude, intensity variation, or corner response thresholds. Although computationally efficient, they often fail with standard thresholds under extreme image transformations, lacking adaptability to changing visibility conditions [8]. Learning based methods aim to learn keypoint detection, description (or sometimes both) but they typically produce sparse keypoints [15]–[19], which are not suitable for computer vision applications that require dense keypoints such as dense 3D reconstruction, AR/VR, and dense Simultaneous Localization and Mapping (SLAM).

A. Classical Detectors and Descriptors

SIFT [12], a powerful scale and rotation invariant algorithm, uses Difference-of-Gaussians for keypoint detection and describes them with gradient-based histograms. SURF [20] is a faster alternative to SIFT that uses integral images and box filters for detection. It also provides feature descriptors but they are less distinctive than SIFT. KAZE [21] detects nonlinear scale-space keypoints directly in the image space yielding highly distinct features but at a higher computational cost whereas AKAZE is accelerated version of KAZE that uses binary descriptors (M-LDB) for faster computation while retaining much of the distinctiveness of KAZE. ORB [22] combines FAST detector with a rotated version of the BRIEF descriptor for speed and rotation invariance.

BRISK [23] uses a circular sampling pattern for detection and generates binary descriptors, offering scale and rotation

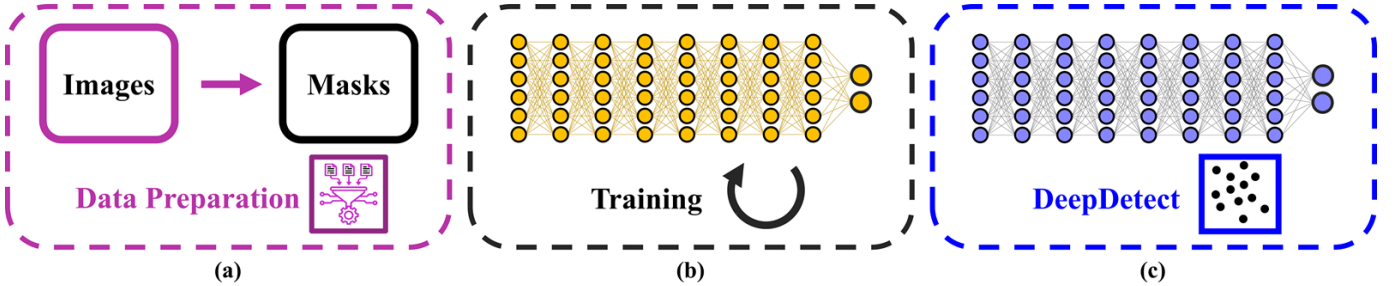


Fig. 3: Main stages in the development of DeepDetect: (a) Fusion masks are created by using 7 keypoint detectors (SIFT, ORB, BRISK, FAST, AGAST, Harris, Shi-Tomasi) and 2 edge detectors (Canny, Sobel) in the images, combining their strengths to capture rich and diverse visual representations. (b) The fused binary masks are then used as labels for the corresponding images to supervise and train ESPNet (a lightweight, efficient model). (c) DeepDetect is ready to detect all-in-one, dense keypoints with semantic awareness and adaptability to complex image degradations, without requiring manual tuning.

invariance with high speed and moderate distinctiveness. FAST [24] is an efficient corner detector that examines a circle of 16 pixels around a candidate keypoint. AGAST [25] is an improvement over FAST, designed to be faster and more robust. Harris Corner Detector (HCD) detects corners by analyzing local intensity changes and Shi-Tomasi Corners focus on stronger minimum eigenvalues, leading to more stable corner detection. Canny [26] is a multi-stage detector that uses gradient computation, non-maximum suppression, and hysteresis thresholding to produce thin and fine edges. Sobel [27] uses convolution with gradient kernels to find edges in the x and y directions, providing thicker edges.

B. Learning based Detection and Description

SuperPoint [15] is a well-known learning based detector and descriptor trained via synthetic homographies, offering high repeatability and descriptor quality across varying conditions. R2D2 [16] learns both repeatability and descriptor reliability via deep learning, filtering out unstable keypoints for robust matching. D2-Net [17] uses a CNN to jointly detect and describe dense keypoints in a single forward pass, particularly effective for challenging photometric and geometric changes. QuadNet is a learning-based detector that uses a quadruplet CNN to learn repeatable and discriminative keypoints without relying on handcrafted heuristics [18]. LIFT [19] learns detection, orientation estimation, and description using three CNNs. Although having some strengths, these algorithms lack semantic awareness about the scenes and do not provide dense keypoints that are especially required in mapping applications such as dense 3D reconstruction, AR/VR, and visual SLAM.

III. DEEPDETECT – METHODOLOGY

A. Data Preparation – Keypoint-Edge Fusion

Data preparation is the first stage towards the development of DeepDetect as shown in Figure 3. We selected 41000 images from the MS-COCO [28] and NewTsukuba [29] datasets, applying extreme reductions in brightness and contrast to 25% of them. Afterwards, they were split into training and validation sets of 33000 and 8000 images, respectively. The strengths of the 7 keypoint detectors and 2 edge detectors are then unified by creating a combined binary mask of their outputs for each image. SIFT detects blob-like structures, while the other 6 keypoint detectors identify corners or ridges. Canny highlights fine details, whereas Sobel captures thicker, high-intensity edges in the images. Binary masks are generated with pixels belonging to the detected keypoints-edges marked as 1 and all other pixels as 0. Extremely low detection thresholds are used for the low visibility scenes, whereas moderate thresholds are used for the normal scenes. This mitigates irrelevant keypoints from the normal scenes while maximizing detection in challenging scenes. For each image, its keypoint and edge masks are merged to create a rich, multi-cue supervision mask that serves as its label during training. Given an image $I \in \mathbb{R}^{H \times W \times 3}$, set of keypoint detectors $D = \{\text{SIFT, ORB, BRISK, FAST, AGAST, Harris, Shi-Tomasi}\}$ and set of edge detectors $E = \{\text{Canny, Sobel}\}$, the final combined mask $M(I)$, shown in Figure 4(d), is obtained as:

$$M(I) = \bigvee_{d \in D} M_d(I) \vee \bigvee_{e \in E} M_e(I) \quad (1)$$

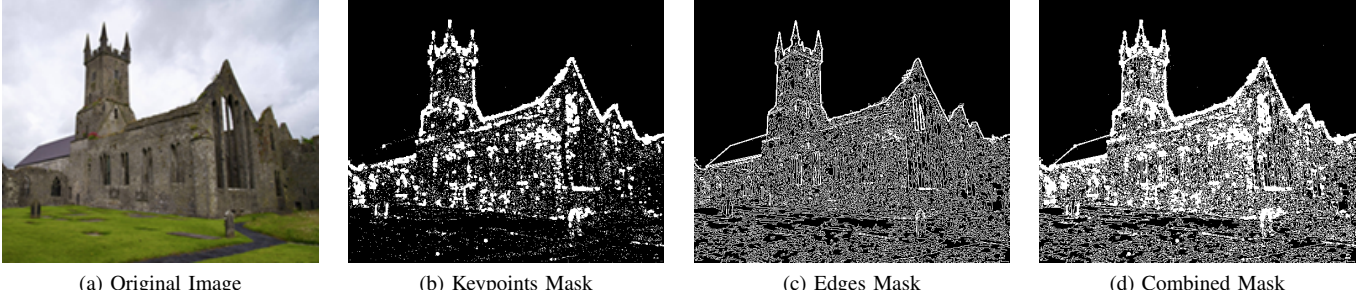


Fig. 4: Binary masks obtained from 7 keypoint and 2 edge detectors, along with their combined version (which provides richer representations for training).

where \vee denotes the pixel wise logical OR operation, $M_D(I)$ shows the fusion mask obtained from the keypoint detectors as in Figure 4(b) and $M_E(I)$ shows the fusion mask obtained from the edge detectors as in Figure 4(c).

B. Learning All-in-One Keypoints – Training Stage

ESPNet [30] is a light weight model designed for highly efficient pixel-wise prediction tasks such as “semantic segmentation” on resource-constrained devices. It has encoder-decoder architecture: the encoder captures contextual information through successive convolution and down-sampling layers while the decoder progressively up-samples the feature maps to restore the spatial resolution. ESPNet is based on ESP modules which factorize the standard convolutions into point-wise (1×1) projections followed by spatial pyramids of dilated convolutions [30]. ESPNet works on a lower dimensional space due to the point-wise projections, reducing its memory footprint and computational cost. Compared to heavy image segmentation models like U-Net [31] and PSPNet [32], it is upto $180 \times$ smaller, $22 \times$ faster, and an excellent choice for low complexity tasks [30].

In the training stage (Figure 3), ESPNet is trained on the prepared dataset for 100 epochs with a learning rate of 0.001 and batch size of 64, using cosine annealing scheduler for smooth convergence. We used Python, OpenCV, and PyTorch [33] for coding. The input image size is kept consistent at $3 \times 480 \times 480$ for the model and its predicted output mask is re-sized to match the spatial dimensions of the original image. Given a target mask $M(I) = y \in \{0, 1\}^{H \times W}$ and model’s raw output $z \in \mathbb{R}^{H \times W}$, the BCE loss $L(y, z)$ is described as:

$$L = -\frac{1}{N} \sum_{i=1}^N \left[y_i \log(\sigma(z_i)) + (1 - y_i) \log(1 - \sigma(z_i)) \right] \quad (2)$$

where σ is the sigmoid function and $N = H \times W$ represents the total number of pixels in the mask. The minimization of loss in Equation 2 encourages the model to produce probabilities closer to 1 for the keypoint pixels and closer to 0 for others. Figure 5 shows the training and validation loss curves of DeepDetect. We picked the model that provided best validation loss during training. During inference, the output z of the model is passed through the sigmoid function to generate the probability $P_p = \sigma(z)$ for pixel p . The predicted output of the model is then thresholded at $\tau = 0.5$ to obtain the final binary mask. The threshold can be adjusted using Equation 3 as per the required keypoint density in the images.

$$M(I) = \begin{cases} 1, & \text{if } P_p \geq \tau \\ 0, & \text{otherwise} \end{cases} \quad (3)$$

C. DeepDetect — Dense Keypoint Detection

DeepDetect is not only learned to reproduce the geometric diversity of the classical keypoint and edge detectors but also able to capture semantically important regions, leading to dense and foreground focused keypoints. To perform image matching, keypoints are first detected in the image pair using

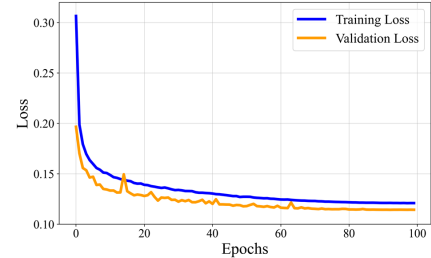


Fig. 5: Training and validation loss curves of DeepDetect.

the trained ESPNet. Afterwards, we use SIFT descriptor to compute the corresponding descriptor vectors, because of its highly distinctive nature. The descriptor sets for the two images are then matched using NNDR based matching. RANSAC can be applied to reject the outliers and filter the correct matches. Qualitative results of DeepDetect are shown in Figure 6. For the comparative analysis presented in Table II and Figure 6, we used the ground-truth Homography matrices [11] (not RANSAC) to obtain the number of correct matches.

IV. EXPERIMENTS & RESULTS

We compare DeepDetect with other keypoint detectors on the Oxford Affine Covariant Regions Dataset [11] using the following evaluation metrics. In all experiments, we used the SIFT descriptor with all the detectors except ORB and BRISK, for which we used their own descriptors.

Keypoint Density: Shows how many keypoints are detected per unit image area. It helps assess whether a detector produces sparse or dense keypoints. Given N detected keypoints in an image with area $H \times W$, the keypoint density is calculated as:

$$\text{Keypoint Density} = \frac{N}{H \times W} \quad (4)$$

Repeatability: Measures the consistency of a detector in finding the same keypoints in images under a given transformation. If N_A and N_B are the number of keypoints detected

TABLE I: Comparison of Average Keypoint Density and Foreground-to-Keypoint (F-KP) Ratio of the Detectors.

Detector	Average Keypoint Density	F-KP Ratio
SIFT	0.0090	0.7606
SIFT (Low)	0.1993	0.3559
ORB	0.0009	0.8508
ORB (Low)	0.1256	0.6797
BRISK	0.0127	0.7909
BRISK (Low)	0.0800	0.5716
FAST	0.0270	0.7442
FAST (Low)	0.3664	0.5387
AGAST	0.0280	0.7363
AGAST (Low)	0.3550	0.5669
Harris	0.0246	0.8262
Harris (Low)	0.2988	0.7389
Shi-Tomasi	0.0052	0.8026
Shi-Tomasi (Low)	0.0326	0.6180
DeepDetect ($\tau = 0.9$)	0.4170	0.7114
DeepDetect ($\tau = 0.8$)	0.4493	0.7113
DeepDetect ($\tau = 0.7$)	0.4733	0.7109
DeepDetect ($\tau = 0.5$)	0.5143	0.7093

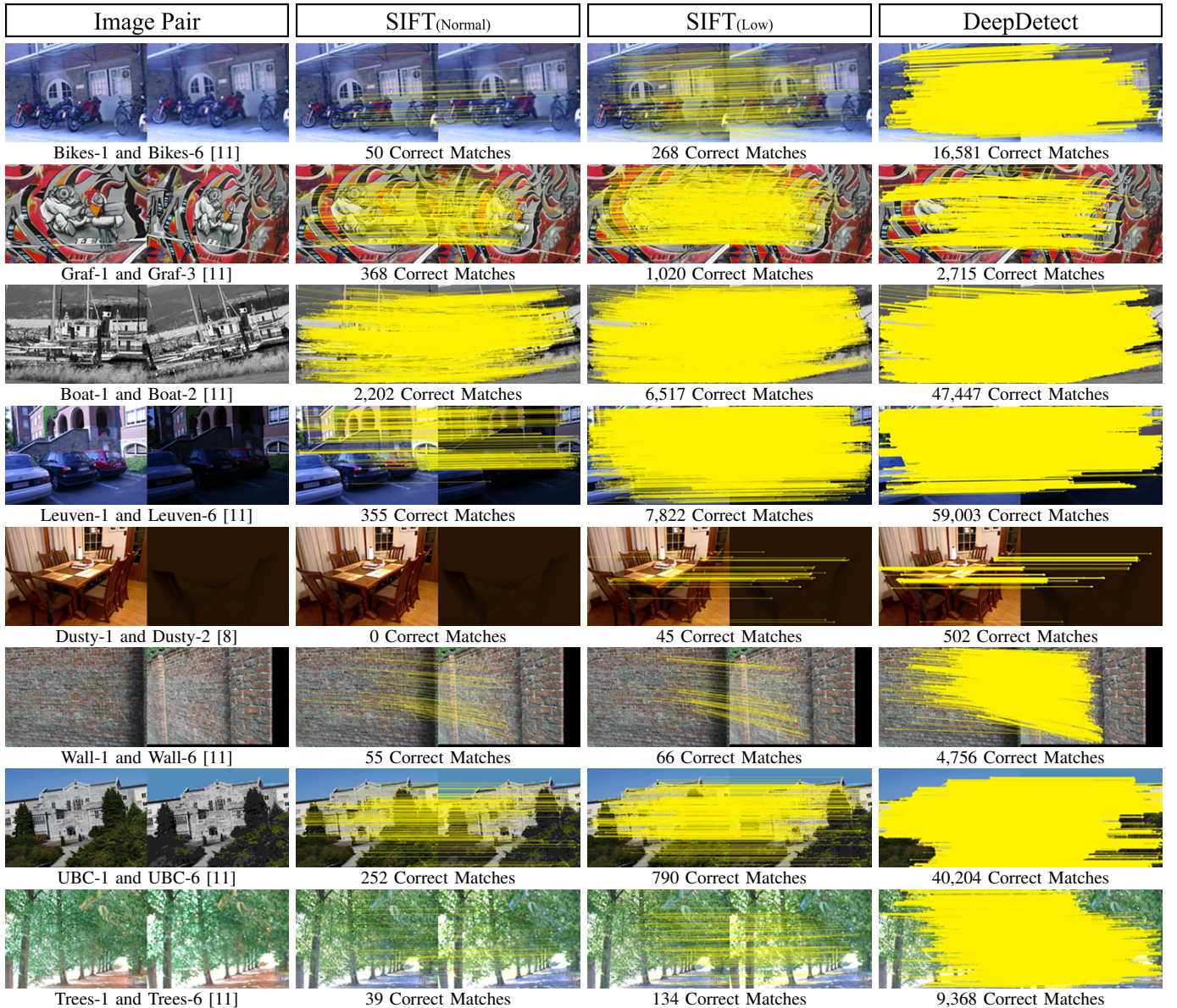


Fig. 6: Qualitative comparison of DeepDetect with SIFT under default and extremely low [8] thresholds. Yellow lines show correct correspondences between the images. DeepDetect provides dense and substantially higher correct matches, without requiring manual tuning (due to its intelligent nature).

in two overlapping images A and B , and $N_{A \cap B}$ is the number of keypoints within the common region $A \cap B$, then:

$$\text{Repeatability} = \frac{N_{A \cap B}}{\min(N_A, N_B)} \quad (5)$$

Foreground-Keypoint (F-KP) Ratio: Evaluates the ability of a detector to detect keypoints within the foreground regions in images. It shows how well a detector focuses on foreground regions rather than the background or irrelevant areas with low or no texture. Let N_F be the number of keypoints in the foreground region and N_T the total detected keypoints, then:

$$\text{Foreground-to-Keypoint Ratio} = \frac{N_F}{N_T} \quad (6)$$

Correct Matches: Higher number of correct matches indicates better performance. If N_A and N_B are the number of

keypoints detected in two overlapping images A and B , then N_C is the number of correct matches between the two sets of keypoints, such that the keypoints of image A are projected onto image B using the ground-truth Homography, and the distance of each keypoint in A to its corresponding keypoint in B is less than a threshold (we used threshold of 1.0 pixel).

Results show that DeepDetect achieves state-of-the-art performance. On Oxford dataset [11], it gives an **average repeatability score** of **0.9582**, surpassing other detectors by a significant margin (see Figure 1). The results for **average keypoint density** are presented in Table I, where DeepDetect achieves the highest average density of **0.5143**. Table I also reports average foreground-to-keypoint ratio on 18 custom-selected images with ground-truth binary masks. DeepDetect achieves good ratios, indicating that its keypoints are not only

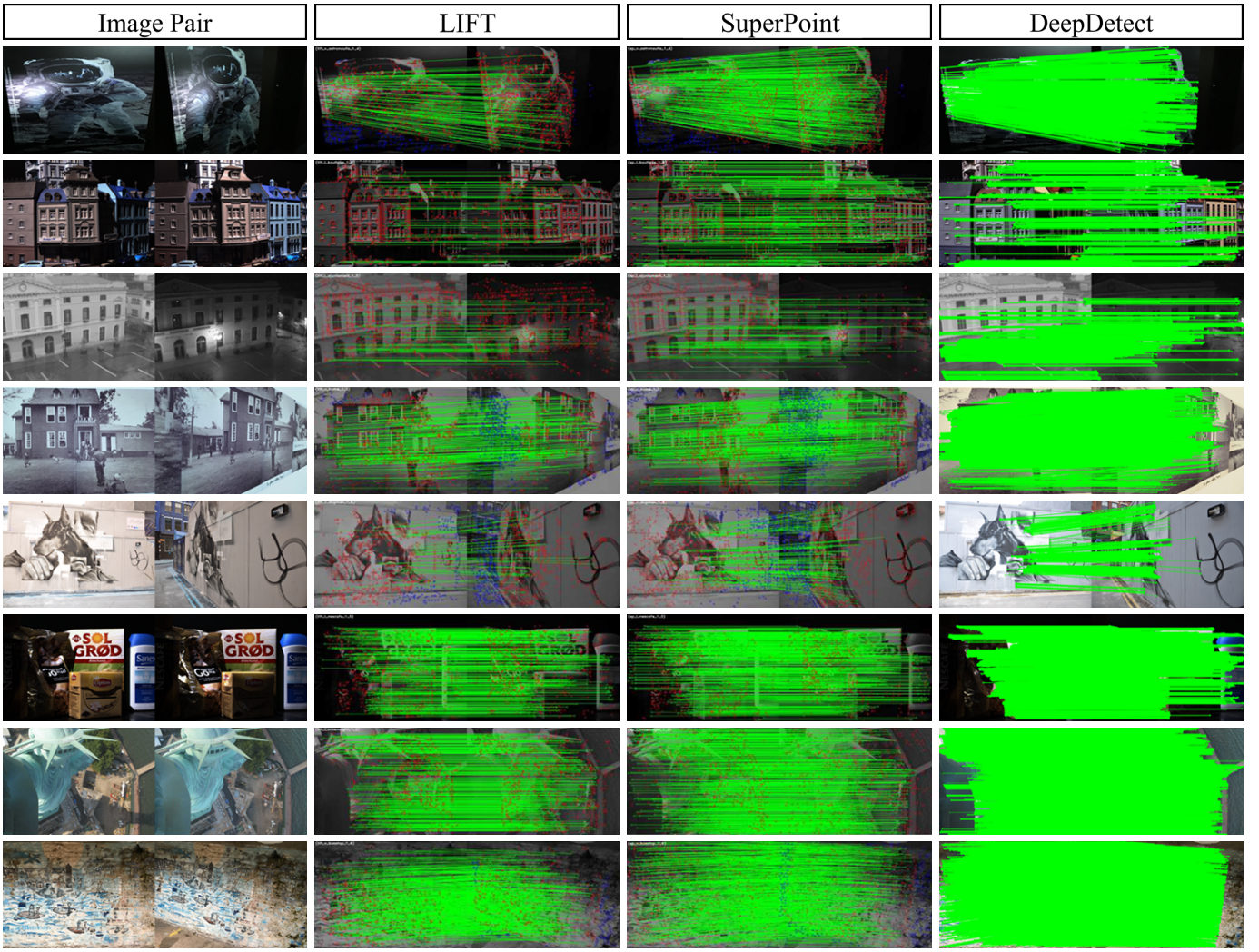


Fig. 7: Qualitative comparison of DeepDetect, LIFT [19], and SuperPoint [15] on HPatches [34]. Green lines show the correct matches between the image pairs: (*astronautis_1_4*, *boutique_1_6*, *ajuntament_1_5*, *home_1_3*, *dogman_1_6*, *nescafe_1_5*, *crownnight_1_2*, *busstop_1_6*). DeepDetect provides dense and substantially higher correct matches across all scenes, achieving over 0.24 million and 0.33 million matches for the final two image pairs, respectively.

TABLE II: Comparison of Correct Matches Produced by Keypoint Detectors for Selected Image Pairs from Oxford dataset [11].

Image Pair	SIFT (Low)	ORB (Low)	BRISK (Low)	FAST (Low)	AGAST (Low)	Harris (Low)	Shi-Tomasi (Low)	DeepDetect
Graf (1–6)	20	5	6	13	5	54	6	102
Boat (1–2)	6517	3749	3836	1703	16238	33385	2164	47447
Wall (1–6)	66	13	14	2156	2357	4270	175	4756
Bikes (1–6)	268	577	358	18112	15458	4652	449	16581
Leuven (1–6)	7822	3582	3163	55427	53972	24296	4159	59003
Trees (1–6)	134	234	181	12078	12185	3834	178	9368
UBC (1–6)	790	977	464	13024	11327	28655	257	40204

dense but also well-concentrated in semantically important regions in the images. With default thresholds, the classical detectors yield higher F-KP ratios but significantly lower keypoint densities. Conversely, reducing thresholds to increase density decreases the F-KP ratio, highlighting the presence of noisy keypoints. For instance, FAST and AGAST with low thresholds, achieve higher densities and lower F-KP ratios, showing their inability to focus salient regions. DeepDetect produces considerably higher densities while maintaining strong foreground focus. Visual comparisons in Figure 2 high-

light how DeepDetect focuses on semantically meaningful regions and provides high keypoint density. Table II and Figure 6 show that DeepDetect provides substantially higher **correct matches** and consistently outperforms classical detectors. As far as learning based algorithms are concerned, Table III shows their **repeatability** comparison with DeepDetect on two different datasets. DeepDetect provides highest repeatabilities due to its intelligent keypoint-edge fusion pipeline. Similarly, Figure 7 shows its qualitative comparison with LIFT and SuperPoint on HPatches, highlighting that DeepDetect outper-

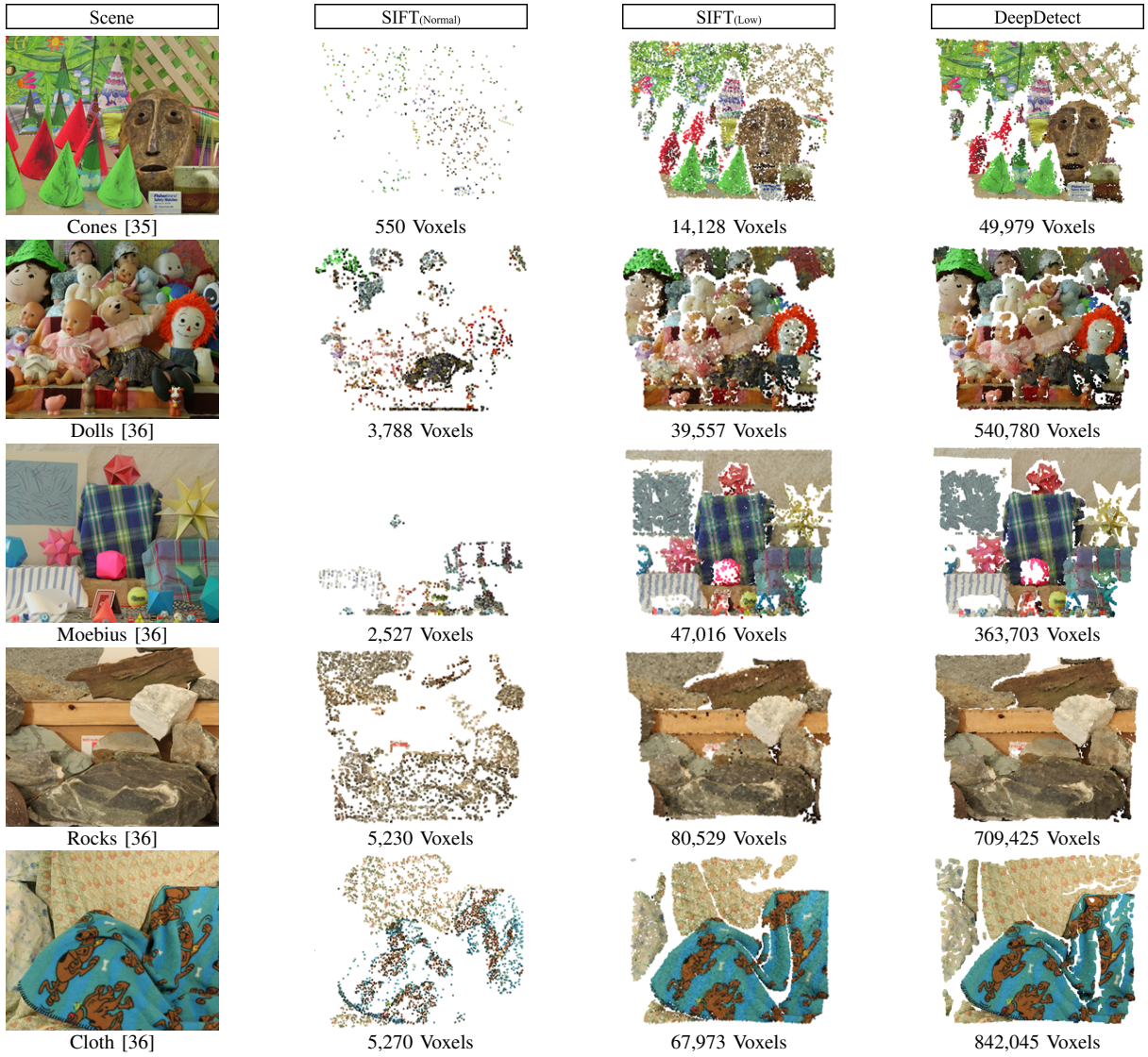


Fig. 8: Comparison of DeepDetect with SIFT for 3D reconstruction (using only two images per scene) on Middlebury datasets [35], [36]. Model used here is trained only on normally illuminated images to avoid low-visibility bias, boosting DeepDetect’s performance for scene geometry. Each row (left to right), shows the left camera image of scene, followed by the 3D reconstructed point clouds using SIFT (default thresholds), SIFT (extremely low thresholds) [8], and DeepDetect. DeepDetect produces highly dense 3D reconstructions, outperforming SIFT even when extremely low thresholds are used.

TABLE III: Comparison of DeepDetect’s repeatability with four well-known learning based detection and description algorithms (MagicPoint [15], SuperPoint [15], QuadNet [18], and R2D2 [16]) on HPatches dataset [34] and Oxford dataset [11].

HPatches Dataset	MagicPoint	SuperPoint	DeepDetect
57 Illumination Scenes	0.575	0.652	0.896
59 Viewpoint Scenes	0.322	0.503	0.901

Oxford Dataset	QuadNet	R2D2	DeepDetect
Graf	0.25	0.47	0.89
Wall	0.46	0.71	0.98
Bark	0.16	0.47	0.91
Boat	0.29	0.57	0.99
Leuven	0.77	0.77	0.99
Bikes	0.57	0.76	0.94
Trees	0.50	0.60	0.95
UBC	0.68	0.68	0.90

forms them with correct matches reaching as high as **338,118** for the *busstop* image pair. To further validate the benefits of DeepDetect, we compare its performance with SIFT (one of the best algorithms) for 3D reconstruction in Figure 8. It is evident that DeepDetect provides high quality, dense 3D reconstructions with number of voxels reaching as high as **842,045**, substantially surpassing the performance of SIFT even when extremely low thresholds are used. The strength of DeepDetect lies in its ability to combine the geometric robustness and diversity of keypoint and edge detectors, and adaptability to extreme image variations gained through the use of supervision masks generated with “different thresholds” for normal and challenging scenes. DeepDetect demonstrates stronger generalization across various conditions without manual tuning due to its **intelligent nature**, making it well suited for visually volatile, changing, or degraded environments.

CONCLUSION

We introduce an intelligent, all-in-one, dense keypoint detector that unifies the strengths of 7 keypoint and 2 edge detectors using deep learning. This keypoint-edge fusion pipeline is called **DeepDetect**. By leveraging keypoint–edge fusion, DeepDetect constructs diverse supervision masks that enable learning of rich, dense, and semantically focused keypoints. Extensive experiments on Oxford, HPatches, and Middlebury datasets demonstrate that DeepDetect outperforms other detectors in repeatability, keypoint density, number of correct matches, and 3D reconstruction quality. DeepDetect can also maintain robustness under extreme image variations depending on the data used for training. Its ability to produce dense, repeatable, and semantically focused keypoints without manual tuning, make it a well suited detector for image matching, 3D reconstruction, visual SLAM, AR/VR, object tracking, and autonomous navigation under visually volatile conditions.

REFERENCES

- [1] K. Mikolajczyk and C. Schmid, “A performance evaluation of local descriptors,” *IEEE transactions on pattern analysis and machine intelligence*, vol. 27, no. 10, pp. 1615–1630, 2005.
- [2] S. Cygert and A. Czyżewski, “Toward robust pedestrian detection with data augmentation,” *IEEE Access*, vol. 8, pp. 136 674–136 683, 2020.
- [3] M. Brown and D. G. Lowe, “Automatic panoramic image stitching using invariant features,” *International journal of computer vision*, vol. 74, no. 1, pp. 59–73, 2007.
- [4] R. Garcia and N. Gracias, “Detection of interest points in turbid underwater images,” in *OCEANS 2011 IEEE-Spain*. IEEE, 2011, pp. 1–9.
- [5] L. Li, J. Lian, L. Guo, and R. Wang, “Visual odometry for planetary exploration rovers in sandy terrains,” *International Journal of Advanced Robotic Systems*, vol. 10, no. 5, p. 234, 2013.
- [6] K. Ebadi, L. Bernreiter, H. Biggie, G. Catt, Y. Chang, A. Chatterjee, C. E. Denniston, S.-P. Deschênes, K. Harlow, S. Khattak *et al.*, “Present and future of slam in extreme underground environments,” *arXiv preprint arXiv:2208.01787*, 2022.
- [7] S. A. K. Tareen and Z. Saleem, “A comparative analysis of sift, surf, kaze, akaze, orb, and brisk,” in *2018 International conference on computing, mathematics and engineering technologies (iCoMET)*. IEEE, 2018, pp. 1–10.
- [8] S. A. K. Tareen and R. H. Raza, “Potential of sift, surf, kaze, akaze, orb, brisk, agast, and 7 more algorithms for matching extremely variant image pairs,” in *2023 4th International Conference on Computing, Mathematics and Engineering Technologies (iCoMET)*. IEEE, 2023, pp. 1–6.
- [9] L. Juan and O. Gwun, “A comparison of sift, pca-sift and surf,” *International Journal of Image Processing (IJIP)*, vol. 3, no. 4, pp. 143–152, 2009.
- [10] E. Karami, S. Prasad, and M. Shehata, “Image matching using sift, surf, brief and orb: performance comparison for distorted images,” *arXiv preprint arXiv:1710.02726*, 2017.
- [11] V. G. Group, “Affine covariant regions datasets,” <http://www.robots.ox.ac.uk/~vgg/data/>, 2004, accessed: Aug. 14, 2025.
- [12] D. G. Lowe, “Distinctive image features from scale-invariant keypoints,” *International journal of computer vision*, vol. 60, no. 2, pp. 91–110, 2004.
- [13] M. A. Fischler and R. C. Bolles, “Random sample consensus: a paradigm for model fitting with applications to image analysis and automated cartography,” *Communications of the ACM*, vol. 24, no. 6, pp. 381–395, 1981.
- [14] O. Chum and J. Matas, “Matching with prosac-progressive sample consensus,” in *2005 IEEE computer society conference on computer vision and pattern recognition (CVPR’05)*, vol. 1. IEEE, 2005, pp. 220–226.
- [15] D. DeTone, T. Malisiewicz, and A. Rabinovich, “Superpoint: Self-supervised interest point detection and description,” in *Proceedings of the IEEE conference on computer vision and pattern recognition workshops*, 2018, pp. 224–236.
- [16] J. Revaud, C. De Souza, M. Humenberger, and P. Weinzaepfel, “R2d2: Reliable and repeatable detector and descriptor,” *Advances in neural information processing systems*, vol. 32, 2019.
- [17] M. Dusmanu, I. Rocco, T. Pajdla, M. Pollefeys, J. Sivic, A. Torii, and T. Sattler, “D2-net: A trainable cnn for joint description and detection of local features,” in *Proceedings of the ieee/cvpr conference on computer vision and pattern recognition*, 2019, pp. 8092–8101.
- [18] N. Savinov, A. Seki, L. Ladicky, T. Sattler, and M. Pollefeys, “Quad-networks: unsupervised learning to rank for interest point detection,” in *Proceedings of the IEEE conference on computer vision and pattern recognition*, 2017, pp. 1822–1830.
- [19] K. M. Yi, E. Trulls, V. Lepetit, and P. Fua, “Lift: Learned invariant feature transform,” in *European conference on computer vision*. Springer, 2016, pp. 467–483.
- [20] H. Bay, A. Ess, T. Tuytelaars, and L. Van Gool, “Speeded-up robust features (surf),” *Computer vision and image understanding*, vol. 110, no. 3, pp. 346–359, 2008.
- [21] P. F. Alcantarilla, A. Bartoli, and A. J. Davison, “Kaze features,” in *European conference on computer vision*. Springer, 2012, pp. 214–227.
- [22] E. Rublee, V. Rabaud, K. Konolige, and G. Bradski, “Orb: An efficient alternative to sift or surf,” in *2011 International conference on computer vision*. Ieee, 2011, pp. 2564–2571.
- [23] S. Leutenegger, M. Chli, and R. Y. Siegwart, “Brisk: Binary robust invariant scalable keypoints,” in *2011 International conference on computer vision*. Ieee, 2011, pp. 2548–2555.
- [24] E. Rosten and T. Drummond, “Machine learning for high-speed corner detection,” in *European conference on computer vision*. Springer, 2006, pp. 430–443.
- [25] E. Mair, G. D. Hager, D. Burschka, M. Suppa, and G. Hirzinger, “Adaptive and generic corner detection based on the accelerated segment test,” in *European conference on Computer vision*. Springer, 2010, pp. 183–196.
- [26] J. Canny, “A computational approach to edge detection,” *IEEE Transactions on pattern analysis and machine intelligence*, no. 6, pp. 679–698, 2009.
- [27] N. Kanopoulos, N. Vasanthavada, and R. L. Baker, “Design of an image edge detection filter using the sobel operator,” *IEEE Journal of solid-state circuits*, vol. 23, no. 2, pp. 358–367, 1988.
- [28] T.-Y. Lin, M. Maire, S. Belongie, J. Hays, P. Perona, D. Ramanan, P. Dollár, and C. L. Zitnick, “Microsoft coco: Common objects in context,” in *European conference on computer vision*. Springer, 2014, pp. 740–755.
- [29] M. Peris, S. Martull, A. Maki, Y. Ohkawa, and K. Fukui, “Towards a simulation driven stereo vision system,” in *Proceedings of the 21st International Conference on Pattern Recognition (ICPR2012)*. IEEE, 2012, pp. 1038–1042.
- [30] S. Mehta, M. Rastegari, A. Caspi, L. Shapiro, and H. Hajishirzi, “EspNet: Efficient spatial pyramid of dilated convolutions for semantic segmentation,” in *Proceedings of the european conference on computer vision (ECCV)*, 2018, pp. 552–568.
- [31] O. Ronneberger, P. Fischer, and T. Brox, “U-net: Convolutional networks for biomedical image segmentation,” in *International Conference on Medical image computing and computer-assisted intervention*. Springer, 2015, pp. 234–241.
- [32] H. Zhao, J. Shi, X. Qi, X. Wang, and J. Jia, “Pyramid scene parsing network,” in *Proceedings of the IEEE conference on computer vision and pattern recognition*, 2017, pp. 2881–2890.
- [33] A. Paszke, S. Gross, F. Massa, A. Lerer, J. Bradbury, G. Chanan, T. Killeen, Z. Lin, N. Gimelshein, L. Antiga *et al.*, “Pytorch: An imperative style, high-performance deep learning library,” *Advances in neural information processing systems*, vol. 32, 2019.
- [34] V. Balntas, K. Lenc, A. Vedaldi, and K. Mikolajczyk, “Hpatches: A benchmark and evaluation of handcrafted and learned local descriptors,” in *Proceedings of the IEEE conference on computer vision and pattern recognition*, 2017, pp. 5173–5182.
- [35] D. Scharstein and R. Szeliski, “High-accuracy stereo depth maps using structured light,” in *2003 IEEE Computer Society Conference on Computer Vision and Pattern Recognition, 2003. Proceedings.*, vol. 1. IEEE, 2003, pp. I–I.
- [36] D. Scharstein and C. Pal, “Learning conditional random fields for stereo,” in *2007 IEEE conference on computer vision and pattern recognition*. IEEE, 2007, pp. 1–8.